WIND POWER SYSTEM BASED ON SQUIRREL CAGE INDUCTION GENERATOR

J. C. Ferreira
Coppe/UFRJ
julio@coe.ufrj.br

I. R. Machado
Coppe/UFRJ
isaac@coe.ufrj.br

E. H. Watanabe
Coppe/UFRJ
watanabe@coe.ufrj.br

L. G. B. Rolim
Coppe/UFRJ
rolim@coe.ufrj.br

***Abstract* – This work presents a study of the wind power system based on Squirrel Cage Induction Generator (SCIG). It also presents an analysis of voltage regulation at the point of common connection (PCC). The induction machine is connected to the grid through a back-to-back PWM controlled voltage source converters (VSC). The induction generator side converter controller (IGSC) is based on field oriented control, while AC side converter controller (ACSC) is based on instantaneous power theory. A 5 hp experimental prototype was developed in Power Electronics Laboratory at COPPE / UFRJ. This prototype will be used to validate the simulated model developed in PSCAD / EMTDC and control strategies.**

***Keywords* – DSP, wind power, induction generator, renewable energy.**

I. INTRODUCTION

The need to reduce the use of greenhouse gas (GHG) emitting energy sources and seek new energy alternatives to meet global energy demand while preserving the planet's natural resources have led to incessant search for renewable power supply. Solar, wind and ocean waves are examples of these types of energy sources. The wind power installed worldwide grew by 1155% between 1997 and 2007 [1], from 7,5 GW to 93,8 GW, with the year 2007 being the most active in the wind power generation history.

The increase of wind energy use in the whole world, particularly in Brazil, encouraged the authors to analyze the impact of wind turbines on voltage quality. This is an actual problem whenever the power coming from the wind is relatively high if compared with the rated power at the point of common connection.

In Brazil, the government has sought incentives for economic development. Among these incentives, there is the PAC (Economic Growth Accelerator Program). This program aims to pursue economic growth and development of the country through investments in infrastructure. However, this economic development is directly related to increased energy demand. Soon, the importance of the participation of wind energy in the Brazilian energy matrix will become significative.

In 2008, the installed wind power in Brazil was 239,25 MW. Currently, in 2011, the installed wind power is 936,78 MW, an increase of over 291% [1]. The Brazilian wind energy potential is estimated 143.5 GW [2]. This growth is linked to PROINFA (Alternative Sources Incentive Program). Initially this program included the installation of a total capacity of 3.3 GW of alternative sources, of which 1.4 GW would correspond to wind energy.

A study of the induction generator control driven by a wind turbine for grid-connected operation using a back-to-back PWM controlled voltage source converter (VSC) was presented in [2]. As the objective was to prove the efficiency of the system, the short-circuit ratio used was very high, so problems such as frequency and voltage regulation were not analyzed.

A study about the control of an induction generator connected to a weak grid by a back-to-back PWM controlled VSC was presented in [3]. The results obtained were very promising. However, in this study the problems of voltage and frequency regulation were not analyzed.

Reference [4] presents an analysis of frequency and voltage regulation in wind diesel systems. A STATCOM with energy storage device was used to improve the frequency and voltage regulation.

The aim of this paper is to present a study of wind power generation system based on a SCIG, emphasizing the voltage quality problem. An experimental prototype was developed at the Power Electronics Laboratory in order to validate the simulated model, which are developed in PSCAD / EMTDC. Sections II and III presents details of the induction generator side and AC side converter control strategies, respectively. Section IV presents discussions on the experimental prototype. The comparative results are presented in section V. The simulated model was used to obtain the frequency response of the system. The PCC RMS voltage frequency also is presented in section V. Section VI presentes the conclusions.

II. AC SIDE CONVERTER CONTROL

Figure 1 shows the wind power system and a block diagram showing the control strategies.

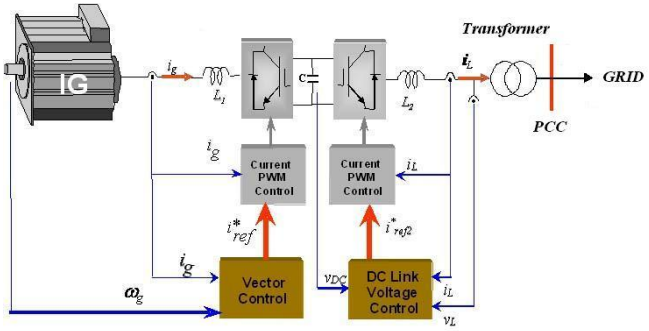

Fig. 1. Wind Power system and control strategies.

The system consists of a SCIG connected to the grid through a back-to-back converter. In the experimental prototype the induction generator is driven by another induction machine (wind turbine emulator). Both machines are rated at 5 hp.

The grid side converter controls the energy flow to the grid. Figure 2 shows the block diagram of this control strategy [5].

The dc capacitor voltage V_{dc} is measured and compared with reference voltage V_{ref}. The difference is fed to a controller that produces an active power reference signal p^*. Due to the controllability aspects, the dc voltage reference voltage is kept 35% above the grid line peak voltage [5-6].

There are some strategies using the reactive power control, however in this work, for simplicity, the reactive power reference is maintained at zero. When the DC link voltage is higher than the reference, a positive signal of active power reference p^* is generated and the energy accumulated in the DC link is transmitted to the grid.

Thus, using the signals p^* and q^* and the instantaneous power theory also known as pq theory [5-8] the converter reference currents $i_{\alpha ref}$ and $i_{\beta ref}$ in α, β reference frame are calculated using:

$$\begin{bmatrix} i_{\alpha ref} \\ i_{\beta ref} \end{bmatrix} = \frac{1}{(v_\alpha^2 + v_\beta^2)} \begin{bmatrix} v_\alpha & -v_\beta \\ v_\beta & v_\alpha \end{bmatrix} \begin{bmatrix} -p^* \\ -q^* \end{bmatrix}, \quad (1)$$

where p^* and q^* are real and imaginary powers references, and v_α e v_β are voltages at the PCC voltages in αβ axis, $i_{\alpha ref}$ and $i_{\beta ref}$ are the currents references.

Reference currents are applied to the current vector control. The measured currents and reference currents are transformed into the dq axis. The angular position of the dq axis is detected using a Phase Locked Loop (PLL). The phase of the positive sequence component of the voltage measured at the PCC is locked. The measured and reference currents are compared and the errors are processed by a PI controller. The output signals of the PI controllers represent voltages signals to be synthesized in the converter terminals [5-6].

III. INDUCTION GENERATOR SIDE CONVERTER CONTROL

Figure 3 presents the block diagram of the induction generator side converter control.

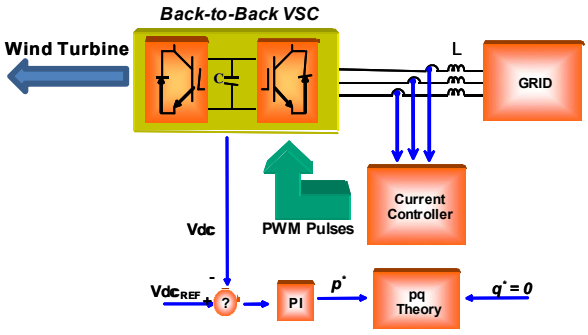

Fig. 2. Block diagram of the dc link voltage control.

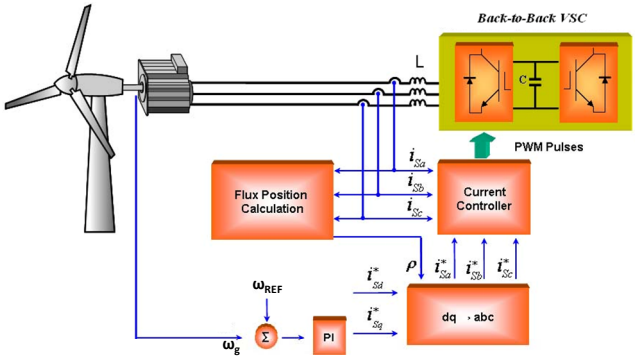

Fig. 3. Block diagram of the generator side converter control.

The control strategy of generator side converter is based on field oriented control [5][9]. In this work, the field reference is the stator magnetic field and its angle is obtained through indirect control method.

The objective is to have the wind turbine operating at or close to the maximum power tracking point [9][10]. For this, the turbine dynamics should be well known.

The mechanical power available in wind is given by:

$$P_{wind} = \frac{1}{2}\rho\pi R^2 v^3, \quad (2)$$

where ρ is the air density, R is the rotor radius and v is the wind speed.

The turbine mechanical power of the wind turbine is given by:

$$P_m = \frac{1}{2}\rho\pi R^2 C_P v^3, \quad (3)$$

where C_p is the turbine power coefficient and v is the wind speed.

Thus, from (2) and (3):

$$P_m = P_{wind} C_P \quad (4)$$

Figure 4 shows the curve relating C_p versus tip speed ratio (λ). A maximum wind power point can be achieved at C_{POPT} if the tip speed ratio is λ_{OPT}.

In Figure 4, tip speed ratio λ represents the ratio between the blade tip speed and wind speed. The optimal turbine speed is given by;

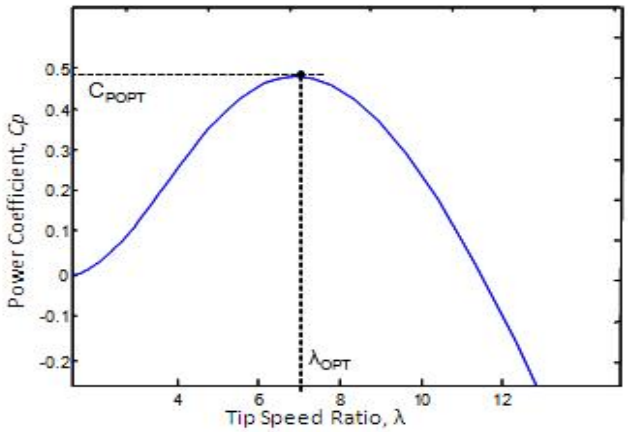

Fig. 4. Typical Cp versus λ curve.

$$\omega_{ref} = \frac{\lambda_{opt} v}{R}. \quad (4)$$

The wind turbine mechanical torque is given by [5][9][10]:

$$T_{tur} = \frac{\frac{1}{2} A \rho v^3 C_p}{\omega_t}, \quad (5)$$

where ω_t is the wind turbine shaft angular speed and A is the wind turbine rotor area.

The mechanical torque applied to the induction generator is give by:

$$T_m = \frac{T_{tur}}{G_R}, \quad (6)$$

where G_R is gear ratio.

The wind turbine emulator is based on this mathematical model.

By measuring the wind speed the IGSC control must ensure that the angular speed of the shaft of the turbine (induction machine) is equal to ω_{ref}, for a given λ_{OPT}, and C_p is maximized, consequently the turbine power is the maximum possible.

An important part of vector control is the rotor magnetic field estimation [5][9]. The algorithm used can be seen in Figure 5.

The electrical torque of the induction machine can be obtained from:

$$m_M(t) = k i_{mR} i_{Sq}. \quad (7)$$

where k is a constant, i_{mR} is the magnetizing current and i_{Sq} is the quadrature component of the current responsible for the torque.

Keeping i_d constant, the electrical torque becomes dependent only on i_{Sq} component, so the machine behavior is approximately linear, like a dc machine.

IV. EXPERIMENTAL PROTOTYPE

Both machine have squirrel cage and are connected by a mechanical shaft. They have same power, 5 hp and same poles number, 2, but only one have a 1024 bit encoder installed. One of them operates as generator and the other as the wind turbine emulator.

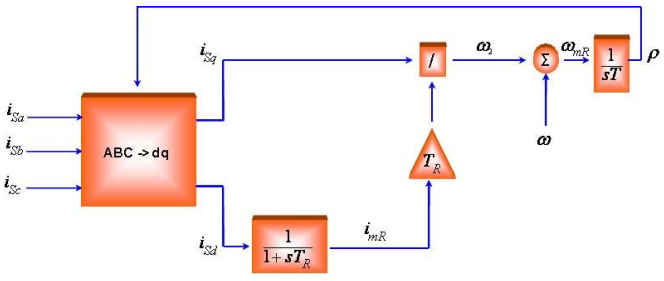

Fig. 5. Magnetic field angle estimation algorithm.

The rated current of the back-to-back PWM controlled voltage source converter (VSC) is 50 A. The IGBT are controlled using optic fiber and they have protection against short-circuit. The dc link capacitance is 4.5 mF and its maximum voltage is 900 V.

The system control have been developed in C program language and it is based on a fixed point DSP controller.

At present, for testing purposes, the torque is defined arbitrarily.

V. RESULTS

Two models were developed in the PSCAD/EMTDC. The first controller simulates the system considering a floating point controller. The other considers a fixed point controller. Both models are based on the system shown in the Fig 1. The experimental prototype was developed based on fixed point DSP. The experimental prototype will be used to validate the simulated results.

The base voltage, current and power values are 311 V, 14.14 A and 3800 W respectively.

The dc link voltage controller is started at t = 0,15 s. The initial wind speed was 11 m/s. At t = 3.0 s, a wind speed step of 1 m/s is applied.

Figures 6 and 7 show the dc link voltage in the simulated model and experimental prototype, respectively.

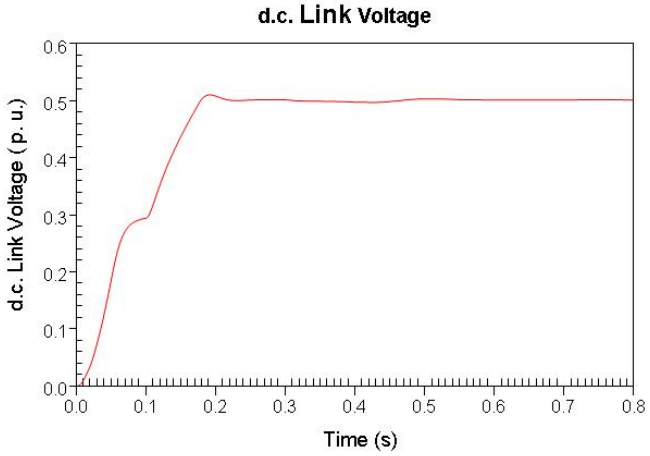

Fig. 6. Simulated dc link voltage.

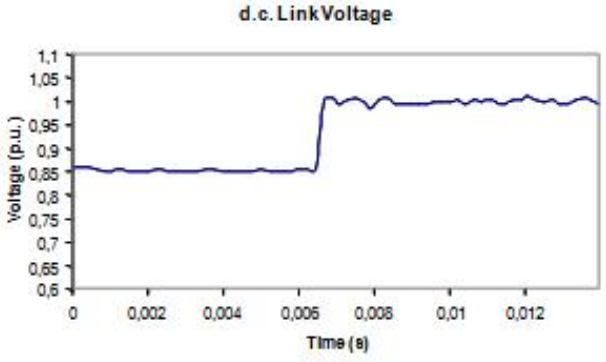

Fig. 7. Experimental prototype dc link voltage.

In Fig. 6 and Fig. 7 we can observe that the grid side converter controller regulates the dc link voltage, wich reference is 400 V.

Figure 8 shows the induction generator speed response simulated using a floating-point control algorithm. In this case the induction generator is driven by a wind turbine, initially, with wind speed equal to 11 m/s. At t = 2.5 s this wind speed is step changed by 1 m/s.

Figure 9 shows the induction generator speed simulated for the case of fixed-point control algorithm. As in the experimental prototype the induction generator is not driven by the turbine emulator yet, in this simulated model, the mechanical torque was not from the wind turbine model, but arbitrarily chosen. The aim is to make the experimental prototype be represented as accurately as possible. Therefore the arbitrary mechanical torque and speed reference were applied. The initial generator speed is 0.41 p.u. At t=1.0 s speed reference is changed to 0.5 p.u.

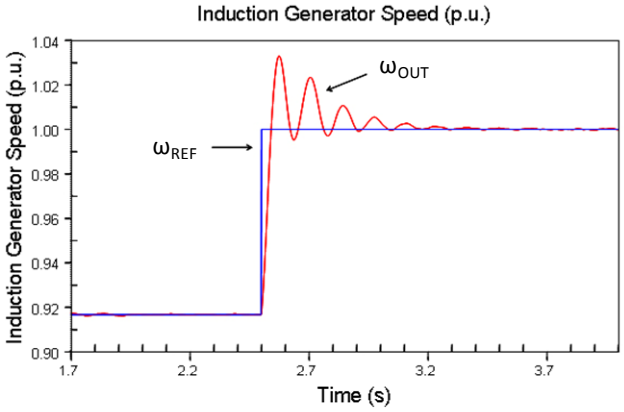

Fig. 8. Induction generator speed simulated response for the floating-point control algorithm wind speed changed from 11 m/s to 12 m/s.

Figure 10 shows the induction generator speed of the experimental prototype. The speed before t=1 was 0.39 p.u. At t=1 a 0.5 p.u. speed reference was applies as the case shown in the Fig 9.

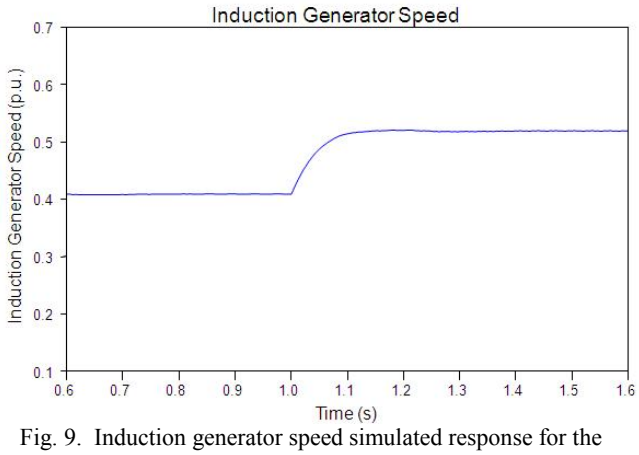

Fig. 9. Induction generator speed simulated response for the case of fixed-point control algorithm.

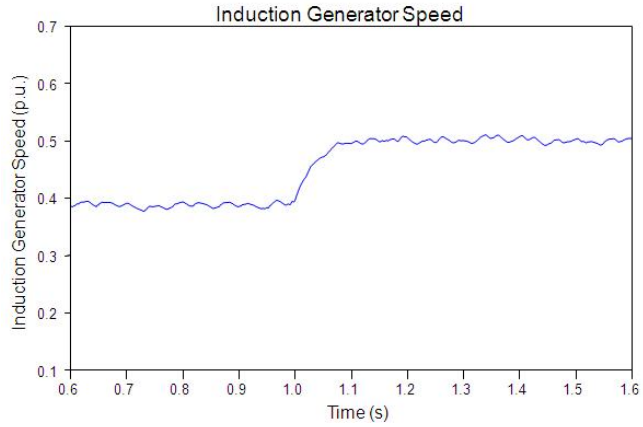

Fig. 10. Induction generator experimental speed response.

The induction generator speed shown in Fig. 9 and Fig. 10 presents an oscillating component. It is caused by quantization problem. One solution to mitigate this problem is to use to a floating point DSP.

Figure 11 shows the power generated by the wind energy system using floating point simulated control algorithm.

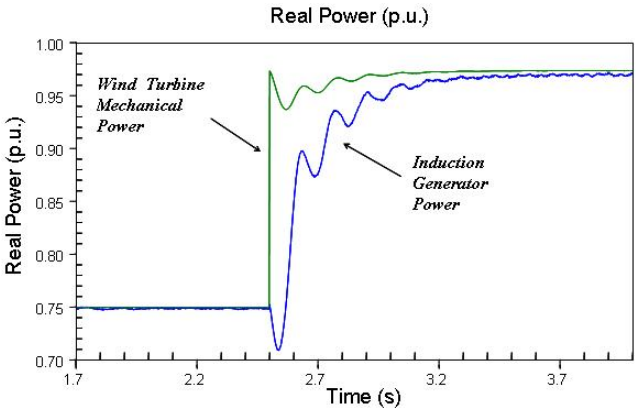

Fig. 11. Power generate by wind energy system simulated response for the floating-point control algorithm

Figures 12 and 13 show the estimated flux position in the fixed point simulated model and in the experimental prototype.

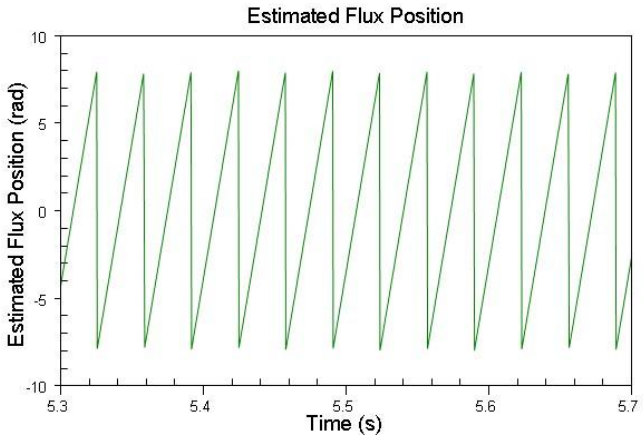

Fig. 12. Simulated estimated flux position for the fixed point DSP control.

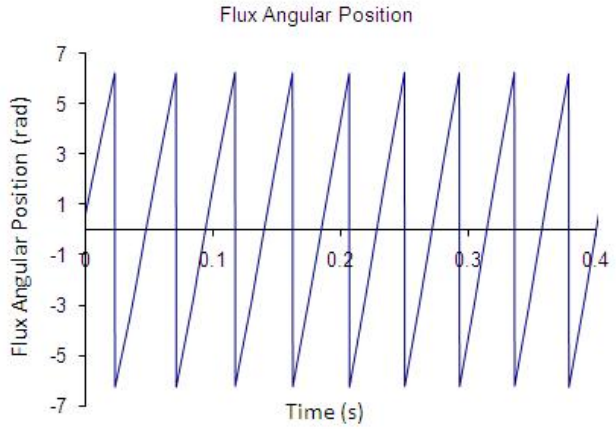

Fig. 13. Estimated flux position at the experimental prototype.

As shown in Fig. 5, induction generator speed is necessary to the estimated flux position algorithm.

VI. ANALYSIS OF VOLTAGE REGULATION AT PCC

Once the computer model has been validated, the next step was to analyze the voltage regulation in PCC due to the wind speed variation.

The wind generation system shown in Fig. 1 was connected to the power grid through an inductance, in order to reduce the short-circuit ratio.

The floating-point simulated model was used to obtain the frequency response of the system. In this case, the short-circuit ratio at the point of common connection was considered 5%, 10%, 30% and 50%. The wind speed was considered as an average value of 11 m/s added with a sinusoidal component with frequency varying from 0.1 Hz to 1 Hz and magnitude from 0.1 m/s to 2 m/s. For each case the PCC rms voltage was measured.

Figures 14 and 15 shows the PCC rms voltage frequency response for the short-circuit ratio of 5% and 10% respectively. It can be observed that for short-circuit ratio at the PCC of 5% and wind speed variations from 0.1 m/s up to 1.9 m/s, the PCC rms voltage variation can reach values from 0.45 % until 0.65 %.

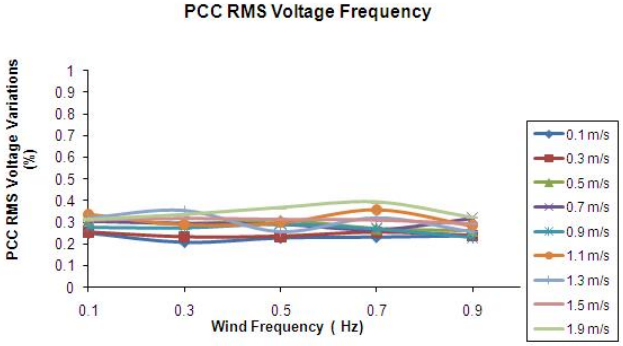

Fig. 14. PCC rms voltage frequency response - short-circuit ratio of 5%.

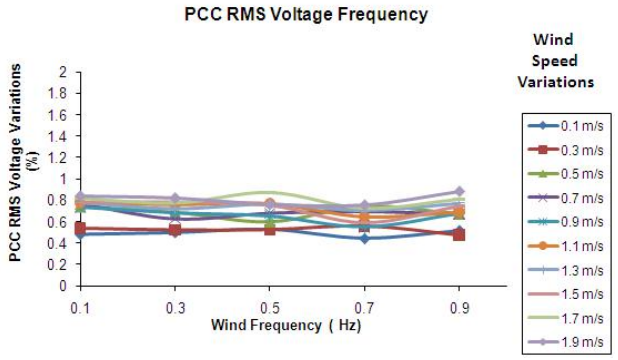

Fig. 15. PCC rms voltage frequency response - short-circuit ratio of 5%.

It can be observed that for short-circuit ratio at the PCC of 10% and wind speed variations from 0.1 m/s up to 1.9 m/s, the PCC rms voltage variation can reach values from 0.85 % until 1.3 %.

Figure 16 shows the PCC rms voltage frequency response for the short-circuit ratio of 30%. In this case, the PCC rms voltage variation can reach values from 7.0 % until 9.5%.

Figure 17 shows the PCC rms voltage frequency response for the short-circuit ratio of 50%. In this case, the PCC rms voltage variation can reach values from 12.0 % until 22.0%.

These conclusions are summarized in Table 1.

TABLE I

short-circuit ratio (%)	Wind Speed Variations (m/s)	PCC RMS Voltage Variation (%)
5	0.1 – 1.9	0.2 – 0.4
10	0.1 – 1.9	0.4 – 0.9
30	1.4 – 2.0	3.0 – 6.0
50	0.1 – 0.6	4.0 – 14.0

VII. CONCLUSION

This works presented a wind energy composed by a squirrel cage induction generator which is connected to the grid through a back-to-back PWM controlled voltage source converter (VSC).system. It also presented an analysis of voltage regulation at the point of common connection (PCC).

The induction generator is driven by another induction machine connected by mechanical shaft and its function was to emulate the wind turbine.

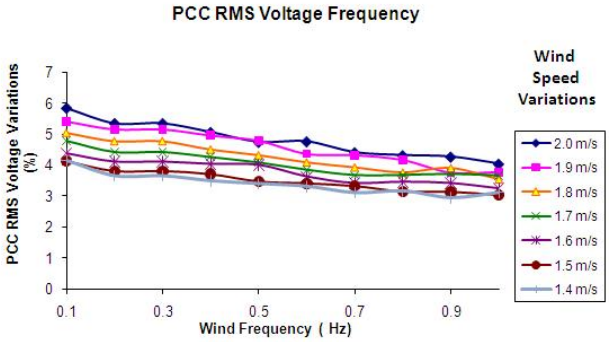

Fig. 16. PCC rms voltage frequency response - short-circuit ratio of 30%.

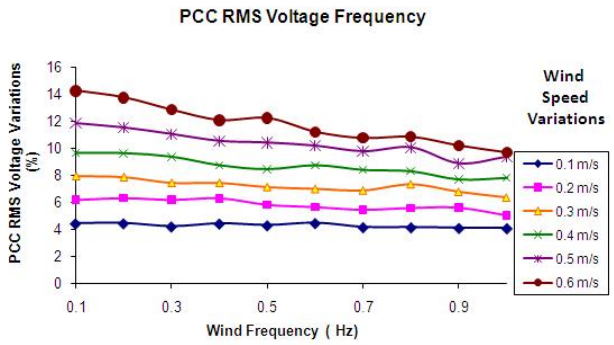

Fig. 17. PCC rms voltage frequency response - short-circuit ratio of 50%.

The control strategy of the converter at the induction generator side is based on field oriented control technique. The objective of this strategy is to allow optimized exploitation of the wind energy.

The control strategy of grid side converter controller is based on instantaneous power theory. The objectives of this strategy are to control the energy flow to the grid.

As stated before it was developed two models in the PSCAD/EMTDC. The first is a floating-point model. The other is a fixed point simulated model. Both the models based on the system shown in the Fig 1. An experimental prototype based was built and tested.

The simulated model was validated by the experimental prototype developed.

The fixed point simulated model was used to obtain the frequency response of the system. The short-circuit ratio at the point of common connection was considered 5%, 10%, 30% and 50%. It was observed that, depending of short-circuit ratio at the PCC ad for the wind speed variations from 0.1 m/s up to 1.9 m/s, the PCC rms voltage variation can reach values from 0.2 % until 14.0 %.

ACKNOWLEDGEMENT

This study received financial support from CNPq, FAPERJ (Cientistas do Nosso Estado) and CAPES / MinCyT.

REFERENCES

[1] http://www.aneel.gov.br/ accessed in July 27, 2011

[2] Ferreira, J. C. C., Moor Neto, J. A. ,Watanabe, E. H., Rolim, L. G. B.,"*Induction Generator Control Driven By a Wind Turbine For Grid Connected Operation Using a Back-to-Back Converter*". In: VI INDUSCON, 2004, Joinvile/SC, 2004.

[3] Ferreira, J. C. C., Moor Neto, J. A., Watanabe, E. H., Rolim, L. G. B., "*Analise de um Controle Utilizando Conversor PWM Back-to-Back para Geradores de Indução Acionados por Turbinas Eólicas*". In: Congresso Brasileiro de Automática, CBA, 2004, Gramado/RS, 2004.

[4] Ferreira, J. C. C., Survire, G., Watanabe, E. H. ; Rolim, L. G. B., Mercado, P." *Active Compensation To Improve Power Quality in Wind/Diesel Generation System*". In: VI INDUSCON, 2006, Recife/PE, 2006.

[5] Barbosa, P. G., Rolim, L. G. B., Watanabe, E. H., Hanitsch, R. (1998). Control strategy for grid-connected DC – AC converters with load power factor correction, *IEE Proc-Gener. Trasm. Distrib.*, Vol. 145, pp. 487-491.

[6] Akagi, H. , Kanazawa, Y., Nabae, A. (1984). Instantaneous reactive power compensators comprising switching devices without energy storage components, *IEEE Trans. Ind. Appl.*, IA-20, (3), pp. 625-630

[7] Watanabe, E. H., Stephan, R. M., Aredes, M. (1993). New concepts of instantaneous active power in electrical systems with generic loads, *IEE Trans. Power Deliv.,* 8, (2), pp. 697-703

[8] Leonhard, W. (1996), *Control of Electrical Drives*, Springer-Verlag, Berlim, Heidelberg.

[9] Hunter, R., Elliot, G. (1994). Wind – Diesel Systems, *A Guide to the Technology and its Implementation*, Cambridge University Press.

[10] Simões, G. M., Farret, F. A., (2004). Renewable Energy Systems, Design and Analysis with Induction Generators, CRC PRESS, Florida.